Electron Mass Enhancement near a Nematic Quantum Critical Point in $NaFe_{1-x}Co_xAs$

C. G. Wang,[1,2] Z. Li,[1,2] J. Yang,[1] L. Y. Xing,[1] G. Y. Dai,[1,2] X. C. Wang,[1] C. Q. Jin,[1,2] R. Zhou,[1] and Guo-qing Zheng[1,2,3]

[1]*Institute of Physics, Chinese Academy of Sciences, and Beijing National Laboratory for Condensed Matter Physics, Beijing 100190, China*
[2]*School of Physical Sciences, University of Chinese Academy of Sciences, Beijing 100190, China*
[3]*Department of Physics, Okayama University, Okayama 700-8530, Japan*

A magnetic order can be completely suppressed at zero temperature (T), by doping carriers or applying pressure, at a quantum critical point, around which physical properties change drastically. However, the situation is unclear for an electronic nematic order that breaks rotation symmetry. Here, we report nuclear magnetic resonance studies on $NaFe_{1-x}Co_xAs$ where magnetic and nematic transitions are well separated. The nuclear magnetic resonance spectrum is sensitive to inhomogeneous magnetic fields in the vortex state, which is related to London penetration depth λ_L that measures the electron mass m^*. We discovered two peaks in the doping dependence of $\lambda_L^2(T \sim 0)$, one at $x_M = 0.027$ where the spin-lattice relaxation rate shows quantum critical behavior, and another at $x_c = 0.032$ around which the nematic transition temperature extrapolates to zero and the electrical resistivity shows a T-linear variation. Our results indicate that a nematic quantum critical point lies beneath the superconducting dome at x_c where m^* is enhanced. The impact of the nematic fluctuations on superconductivity is discussed.

In the high transition-temperature (T_c) superconducting cuprates or iron pnictides, superconductivity adjoins a magnetically ordered phase [1,2]. With increasing carrier doping or externally applied pressure to a parent phase, the magnetic order is suppressed and a superconducting phase emerges. The magnetic order temperature T_N goes to zero before superconductivity appears or extrapolates to zero at a point inside a superconducting dome. Around the ending point of $T_N = 0$, namely, a quantum critical point (QCP), many anomalous physical properties due to the associated quantum fluctuations have been revealed by various experimental methods [3–6]. A magnetic QCP is considered by many a key to understanding the mechanism of high-T_c superconductivity [7]. For example, the electron pairing strength is believed to be enhanced by the magnetic quantum fluctuations [8].

In iron pnictides, in addition to the magnetic order, there also exists an electronic nematic order that breaks rotation symmetry, setting in at the tetragonal-to-orthorhombic structural transition temperature T_s or even above [5,9–11], which has attracted much attention recently. It was proposed that such nematic order may stem from the electronic orbital degree of freedom, in addition to the spin degree of freedom [12–14]. Thus, the electronic nematicity points to a new frontier of condensed matter physics [15,16] and may also hint at a possible new route to high-T_c superconductivity [17–19]. Although some anomalous physical properties such as temperature (T)-linear electrical resistivity or diverging nematic susceptibility behavior can be understood as being due to

nematic quantum fluctuations at high temperatures [6,12,20], a direct evidence for a nematic QCP inside the superconducting dome is still lacking.

If a QCP is indeed hidden inside the dome, it would manifest itself in some physical quantities that describe the zero-T-limit properties. London penetration depth λ_L is determined by the superfluid density n and the effective mass m^* of carriers responsible for superconductivity [21], and $\lambda_L(T = 0)$ can be a good tool for probing a hidden QCP. This is because many experiments indicated that m^* can be enhanced due to quantum fluctuations [4,22,23]. In the cuprate superconductor $YBa_2Cu_3O_{6+\delta}$, as the magnetic QCP is approached from the underdoped side, m^* increased by a factor of 3 [22]. In the isovalent-doped Fe-based superconductor $BaFe_2(As_{1-x}P_x)_2$, a sharp peak of $\lambda_L(0)$ was indeed found at the optimal doping concentration $x = 0.3$, which was attributed to an antiferromagnetic QCP [4]. Quantum oscillation measurements confirmed that upon decreasing x from 0.8 to 0.3, m^* is doubled [23].

In the iron pnictides, the putative magnetic QCP and electronic nematic QCP are usually close by or even indistinguishable, which hindered the progress of experimental investigations on the later. $NaFe_{1-x}Co_xAs$ is an exceptional system [24] whose T_s is about 10 K higher than T_N in the parent undoped compound. With Co doping, T_N is suppressed much more rapidly than T_s. The difference between the two transitions increases to 20 K at $x = 0.018$ [11]. In the orthorhombic phase, electronic nematicity was visualized in the parent compound by scanning tunneling microscopy [9], and both orbital and spin nematicity were

observed above T_s by nuclear magnetic resonance (NMR) [11].

The Co-doping concentration to obtain the highest T_c is only $\sim 2.7\%$, that is, much smaller than any other systems [24]. As demonstrated by the much narrower ^{75}As-NMR lines [25], the doping-induced disorder in the FeAs plane, which is usually harmful to a QCP, is much less compared to other systems. These advantages provide one a unique opportunity to explore a nematic QCP and its influence on the physical properties.

In this Letter, through ^{23}Na NMR spectrum measurements, we present a detailed study of $\lambda_L^2(T \sim 0)$ in NaFe$_{1-x}$Co$_x$As ($0.0089 \leq x \leq 0.056$). The single crystals were grown by the self-flux method [9]. Experimental details can be found in Ref. [11]. The Co content x was checked by the ^{23}Na-NMR Knight shift (see Fig. S1 [25]). The ^{23}Na NMR spectra were obtained by fast Fourier transform of the spin echo. We find two peaks in the doping dependence of $\lambda_L^2(T \sim 0)$, one at $x_M = 0.027$, and the other at $x_c = 0.032$.

In the vortex state, the magnetic field B_0 penetrates into a sample in the unit of quantized flux $\phi_0 = 2.07 \times 10^{-15}$ T m^2, so the field becomes inhomogeneous. For $B_{c1} \ll B_0 \ll B_{c2}$, where B_{c1} and B_{c2} are the lower and upper critical field, respectively, the field distribution $\triangle B$ can be written as [36]

$$\Delta B = 0.0609 \frac{\phi_0}{\lambda_L^2}, \tag{1}$$

which can be detected by the ^{23}Na- or ^{75}As-NMR spectrum broadening $\Delta f = \gamma_n \triangle B$, where γ_n is the gyromagnetic ratio. In our case, $B_{c1} < 0.005$ T and $B_{c2} > 44$ T for $0.02 < x < 0.05$ [37]. The ^{23}Na-NMR spectrum is much narrower than that of ^{75}As-NMR [38], and thus has a higher resolution for determining λ_L.

Figure 1 shows the ^{23}Na-NMR spectra for various samples, and the T dependence of the spectrum for $x = 0.032$. In the normal state, the spectrum is well fitted by a single Lorentz function with a full width at half maximum (FWHM) of about 4 kHz at $B_0 = 12$ T. The almost same width is obtained for other samples [25], which indicates high sample quality. In the superconducting state, the spectrum is broadened nearly symmetrically and is also a Lorentzian [25]. Since the FWHM of a convolution of two Lorentzian functions is the sum of individual FWHMs, the broadening can be obtained by simply subtracting the T-independent width, $\Delta f =$FWHM(T)-FWHM$(T > T_c)$ [25].

Theoretically, the field distribution due to the vortex-lattice formation should introduce an asymmetric broadening so that a "Redfield pattern" will be observed. However, such a pattern is seldom seen in correlated systems except for limited examples [39–42]. In the current case, no clear Redfield pattern is observed down to $B_0 = 3$ T. The symmetric line shape is likely due to flux-line oscillations along the c axis which creates a vortex-lattice disorder between different layers [43].
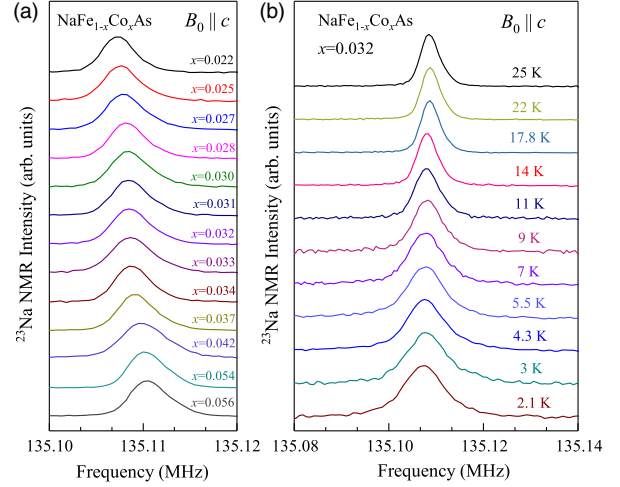

FIG. 1. (a) The ^{23}Na spectra for $0.022 < x < 0.056$ in the normal state ($T = 25$ K) at $B_0 = 12$ T. (b) Typical temperature evolution of the ^{23}Na spectra for the $x = 0.032$ sample at $B_0 = 12$ T.

Indeed, a symmetric magnetic-field distribution was observed in Bi$_2$Sr$_2$CaCu$_2$O$_6$ by muon spin rotation and explained by such "disordered fluxon model" [44].

In order to experimentally demonstrate that Eq. (1) is indeed valid, we show the shift and Δf at various fields in Fig. 2. A field-independent Δf is clearly seen as expected by the London theory for $B_0 > B_{c1}$, indicating that the broadening is indeed caused by the vortices. Additional evidence for the broadening stemming from the vortex lattice is that the shift is progressively reduced with a decreasing field. Such diamagnetism is solid evidence for vortex-lattice formation. The diamagnetic shift $^{23}K_{\text{dia}}(B_0)$ is also related to λ_L as [45]

$$^{23}K = {}^{23}K_0 + {}^{23}K_{\text{dia}}(B_0)$$
$$= {}^{23}K_0 - (1 - D) \frac{\phi_0}{8\pi \lambda_L^2 B_0} \ln\left(\frac{4\pi\beta^2}{e\sqrt{3}} \frac{B_{c2}}{B_0}\right), \tag{2}$$
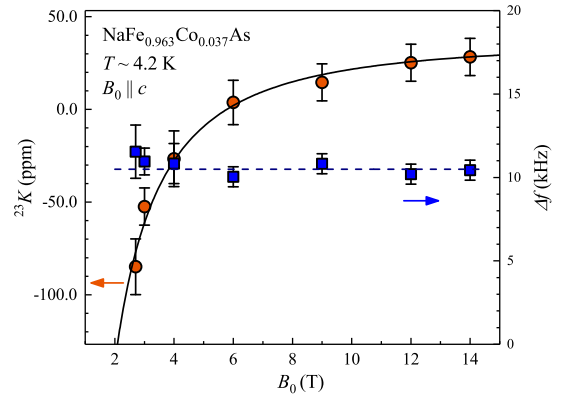
FIG. 2. Field dependence of ^{23}K and line broadening $\Delta f =$ FWHM$(T = 4.2$ K$)$-FWHM$(T = 25$ K$)$ for the $x = 0.037$ sample. Solid curve is a fitting to Eq. (2) by taking $D = 0.8$. The dashed line is a guide for the eyes.
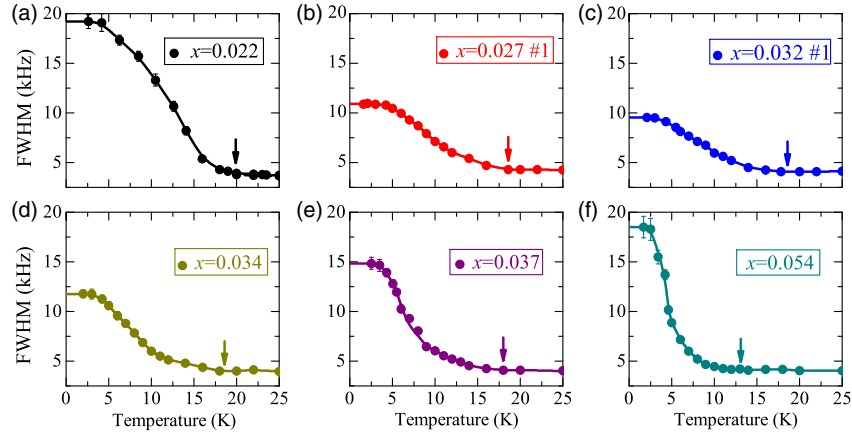
FIG. 3. Temperature dependence of the full width at half maximum (FWHM) of the ^{23}Na-NMR spectra for various doping concentrations. The arrow indicates T_c at $B_0 = 12$ T.

where D is the demagnetization factor which is 0.8 for $x = 0.037$ [46], and $\beta = 0.38$ for triangular lattice. It has been shown previously that ^{23}K is T independent below 100 K, although ^{75}K is strongly T dependent [38], which is confirmed by our measurements. This result indicates that the contribution from spin susceptibility to ^{23}K is negligible. Then we fitted ^{23}K to Eq. (2) and obtained $\lambda_L = 0.35 \pm 0.03$ μm and $B_{c2} = 60 \pm 20$ T. Such obtained λ_L is in fair agreement with $\lambda_L(0) = 0.367$ μm obtained from Eq. (1) (see below). The deduced B_{c2} is also consistent with the previous report of $B_{c2} > 44$ T [37]. For $x = 0.03$ at $B_0 = 4$ T, we have also confirmed that ^{23}K becomes negative (~ -30 ppm) [25]. All these assure that Eq. (1) is applicable.

Figure 3 shows the T dependence of the FWHM. For all samples, the broadening saturates below $T_{\text{sat}} = 0.2$–0.4 T_c, indicating a fully opened superconducting gap, which is consistent with the ARPES result [47,48]. Then, $\lambda_L^2(0)$ is obtained according to Eq. (1) using the data below T_{sat}, with the results summarized in Fig. 4(a). The results obtained at $B_0 = 4$ T for $x = 0.03$ and 0.037 agree well with those at $B_0 = 12$ T [25], which again assures that Eq. (1) is valid for our case. The three data points in the figure previously reported by muon spin rotation [49] and by surface impedances [50] measurements are in good agreement with our data.

A peak is observed in the doping dependence of $\lambda_L^2(0)$ at $x_M = 0.027$. In addition, and most remarkably, an even higher peak is observed at $x_c = 0.032$. A possibility of mesoscopic phase separation that might be responsible for an enhancement of $\lambda_L^2(0)$ [51] can be ruled out, as the NMR linewidth at $T = 25$ K shows no anomaly at $x = 0.027$ and 0.032 (see Fig. S9 in the Supplemental Material [25]).

In a clean single crystal, $\lambda_L^2(0)$ is related to the electron mass as [21]

$$\lambda_{\text{L}}^{-2}(0) = \mu_0 e^2 \sum_i n_i/m_i^*, \qquad (3)$$
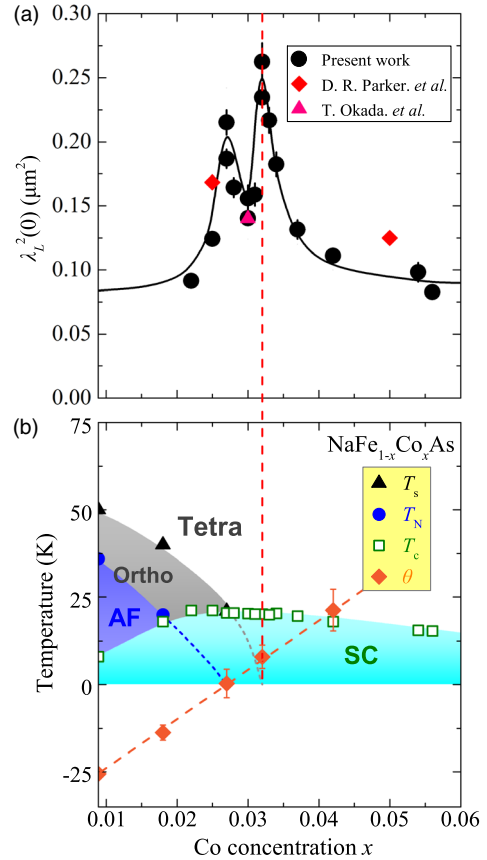

FIG. 4. (a) x dependence of the squared London penetration depth $\lambda_L^2(0)$. For $x = 0.027$, 0.03, and 0.032, two samples were measured. The sample indicated by no. 1 in Fig. 3 corresponds to a larger $\lambda_L^2(0)$. The red diamonds and triangle are from previous reports by other methods [49,50]. The curve is a guide to the eyes. (b) The obtained phase diagram of NaFe$_{1-x}$Co$_x$As. The T_N and T_s are obtained from the previous NMR spectra [11]. AF and SC denote antiferromagnetic ordered and superconducting phase, respectively. Ortho and tetra denote the orthorhombic and tetragonal crystal structure, respectively. The parameter θ is obtained from the $1/T_{1c}T$ data (see text).

where μ_0 is the vacuum magnetic permittivity, e is the electron charge, m_i^* and n_i are, respectively, the effective mass and the superconducting carriers density in band i. Therefore, a peak of $\lambda_L^2(0)$ is an indication of strong enhancement of the effective mass m^*, as n_i changes monotonically with x [25]. In $BaFe_2(As_{1-x}P_x)_2$, a peak in $\lambda_L^2(0)$ was found and attributed to the existence of a magnetic QCP [4], although theoretical interpretation was controversial [51–54]. As we elaborate below, the first peak indicates that a magnetic QCP lies beneath the superconducting dome at $x_M = 0.027$, while the higher peak indicates that an electronic nematic QCP lies beneath the dome at $x_c = 0.032$.

We measured the spin-lattice relaxation rate $^{75}(1/T_{1c})$ with the magnetic field B_0 along the c axis. The quantity $^{75}(1/T_{1c}T)$ consists of two contributions, $^{75}(1/T_{1c}T) = {}^{75}(1/T_{1c}T)_{AF} + {}^{75}(1/T_{1c}T)_{intra}$, where the former represents the contribution from antiferromagnetic spin fluctuations and the latter from an intraband effect [6,55]. The $^{75}(1/T_{1c}T)_{AF}$ follows a Curie-Weiss behavior $b/(T + \theta)$, as expected for a two-dimensional system near a magnetic QCP [56]. The $^{75}(1/T_{1c}T)_{intra}$ is due to the density of states at the Fermi level, which is related to the spin Knight shift K_s according to the Korringa relation [57]. As shown in Fig. 5(b), the Knight shift can be fitted by $^{75}K = {}^{75}K_0 + {}^{75}K_1 \exp(-E_g/k_BT)$, where $^{75}K_0$ is a constant and $^{75}K_1$ is a T-dependent spin Knight shift. Then we can fit the data by $^{75}(1/T_{1c}T) = a + b/(T + \theta) + c \exp(-2E_g/k_BT)$ to deduce θ as have been done in $BaFe_{2-x}[Co, Ni]_xAs_2$ [6,55]. The obtained parameter θ is plotted in Fig. 4. The value of θ is almost zero for $x_M = 0.027$, which means that the staggered susceptibility is governed by a magnetic QCP to become diverging at $T = 0$ [56]. In order to see this more visually, we plot $^{75}(1/T_{1c})_{AF}$ in Fig. 6. For $x_M = 0.027$, $^{75}(1/T_{1c})_{AF}$ is almost T independent, which intuitively demonstrates that the system shows a quantum critical behavior. The T-linear resistivity supports this conclusion (see Fig. S12 in the Supplemental Material [25]). We emphasize that $1/T_1$ and the resistivity are high-T fingerprints of the magnetic QCP, while the peak of $\lambda_L^2(0)$ is the direct evidence of QCP at the zero-T limit. In passing, we note that the previous result on $BaFe_2(As_{1-x}P_x)_2$ [4] has created theoretical debates on its interpretation [51–54]. Chowdhury et al. warned that a phase separation could give rise to a decrease of superfluid density, thereby resulting in an increasing of $\lambda_L^2(0)$ [51]. This was indeed the case in the $LaFeAsO_{1-x}F_x$ system [58], where phase separation was made evident by nuclear quadrupole resonance measurements [59]. However, as mentioned above, no indication of phase separation was seen in our samples by ^{23}Na or ^{75}As NMR spectra [11,25]. Our result therefore indicates that indeed a magnetic QCP can give rise to mass enhancement.

On the other hand, $x_c = 0.032$ is clearly far from $x_M = 0.027$, and thus the mass enhancement there is *not*
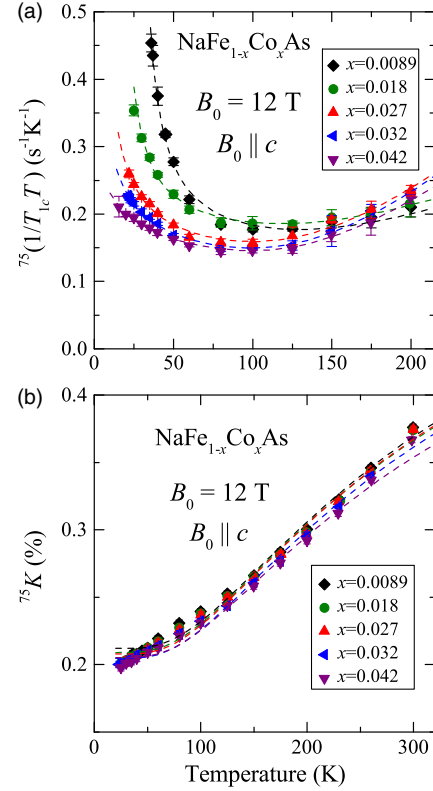

FIG. 5. (a) T dependence of $^{75}(1/T_{1c}T)$ for various $NaFe_{1-x}Co_xAs$. The dashed curves are a fit of $^{75}(1/T_1T)$ to $^{75}(1/T_1T) = a + b/(T + \theta) + c \exp(-2E_g/k_BT)$ (see text), with the obtained θ plotted in Fig. 4. (b) T dependence of ^{75}K for various $NaFe_{1-x}Co_xAs$. The dashed lines are a fit of ^{75}K to $^{75}K = {}^{75}K_0 + {}^{75}K_1 \exp(-E_g/k_BT)$ (see text).

related to the magnetic QCP. We note that T_s extrapolates to zero around $x_c = 0.032$ [11], at which the electrical resistivity also shows a good T-linear behavior up to $T = 110$ K (see Fig. S12 in the Supplemental Material [25]).
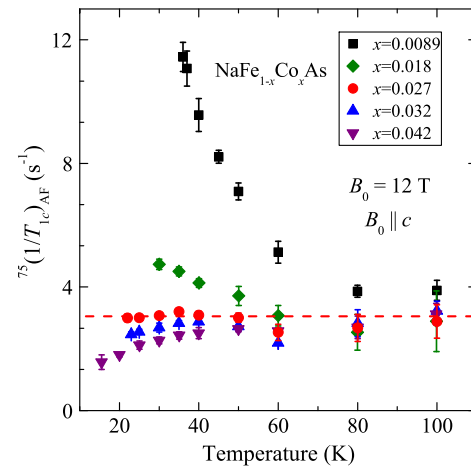

FIG. 6. The T and x dependencies of $1/T_1$ due to antiferromagnetic spin fluctuations. The T-independent $1/T_1$ indicates a magnetic QCP.

This result together with previous NMR [11] and Raman [60] studies suggests that nematic fluctuations [20,61] exist above the superconducting dome. We conclude that the peak we observed at $x_c = 0.032$ is evidence that a nematic QCP lies *beneath* the superconducting dome, where the mass is enhanced by a factor ~ 2.5 due to a band renormalization caused by quantum nematic fluctuations. It was theoretically shown by a Monte Carlo calculation that a nematic quantum fluctuations can lead to an enhancement of a factor ~ 4 [20].

The existence of a nematic QCP seems to affect superconductivity of this system. In $BaFe_2(As_{1-x}P_x)_2$ where x_M and x_c are too close or indistinguishable, there is a well-defined maximum in the doping dependence of T_c. In striking contrast, T_c of $NaFe_{1-x}Co_xAs$ shows a weak decrease for $x \geq 0.027$, as seen in Fig. 4(b). This suggests that nematic fluctuations play a role in enhancing the pairing interaction. It is believed by many that superconductivity at the low doping region is mediated by spin fluctuations with large momentum q. We speculate that nematic fluctuation with $q \sim 0$ helps enhance pairing interaction as to prevent T_c from a rapid decrease for $x > 0.027$ where spin fluctuations are weakened. The same is probably true in the second dome of $LaFeAsO_{1-x}F_x$ ($0.3 < x < 0.8$), where spin fluctuations are weak but T_c is higher than that in the first dome ($0 < x < 0.25$) [17]. Our results provide strong motivations for further investigations in this regard. Also, it would be a good future task to investigate how the pairing symmetry changes when nematic fluctuations are weakened at large x where T_c decreases.

Meanwhile, in $YBa_2Cu_3O_y$, quantum oscillation shows that the effective mass is enhanced around the optimal doping [22], where the rotation symmetry was found to be broken [62–64], which suggests that there also exists a QCP with nematic character. Therefore, our results suggest a possible link between the two different classes of the high-T_c superconductors and will stimulate more studies on the cuprates.

In summary, we have systematically studied the zero-T-limit London penetration depth $\lambda_L^2(0)$ in $NaFe_{1-x}Co_xAs$ to diagnose the quantum critical behavior inside the superconducting dome. A nematic QCP is found inside the superconducting dome at $x_c = 0.032$, which is clearly distinguished from the magnetic QCP $x_M = 0.027$. Our results indicate that the electron mass is enhanced near the nematic QCP due to band renormalization by nematic quantum fluctuations.

[1] P. A. Lee, N. Nagaosa, and X. G. Wen, Rev. Mod. Phys. **78**, 17 (2006).
[2] G. R. Stewart, Rev. Mod. Phys. **83**, 1589 (2011).
[3] P. Gegenwart, Q. Si, and F. Steglich, Nat. Phys. **4**, 186 (2008).
[4] K. Hashimoto, K. Cho, T. Shibauchi, S. Kasahara, Y. Mizukami, R. Katsumata, Y. Tsuruhara, T. Terashima, H. Ikeda, M. A. Tanatar, H. Kitano, N. Salovich, R. W. Giannetta, P. Walmsley, A. Carrington, R. Prozorov, and Y. Matsuda, Science **336**, 1554 (2012).
[5] J. H. Chu, H. H. Kuo, J. G. Analytis, and I. R. Fisher, Science **337**, 710 (2012).
[6] R. Zhou, Z. Li, J. Yang, D. L. Sun, C. T. Lin, and G.-q. Zheng, Nat. Commun. **4**, 2265 (2013).
[7] P. Coleman and A. J. Schofield, Nature (London) **433**, 226 (2005).
[8] T. Moriya and K. Ueda, Adv. Phys. **49**, 555 (2000).
[9] E. P. Rosenthal, E. F. Andrade, C. J. Arguello, R. M. Fernandes, L. Y. Xing, X. C. Wang, C. Q. Jin, A. J. Millis, and A. N. Pasupathy, Nat. Phys. **10**, 225 (2014).
[10] T. Iye, M. H. Julien, H. Mayaffre, M. Horvatic, C. Berthier, K. Ishida, H. Ikeda, S. Kasahara, T. Shibauchi, and Y. Matsuda, J. Phys. Soc. Jpn. **84**, 043705 (2015).
[11] R. Zhou, L. Y. Xing, X. C. Wang, C. Q. Jin, and G.-q. Zheng, Phys. Rev. B **93**, 060502 (2016).
[12] H. H. Kuo, J. H. Chu, J. C. Palmstrom, S. A. Kivelson, and I. R. Fisher, Science **352**, 958 (2016).
[13] R. M. Fernandes and J. Schmalian, Phys. Rev. B **82**, 014521 (2010).
[14] H. Kontani and S. Onari, Phys. Rev. Lett. **104**, 157001 (2010).
[15] A. Chubukov and P. J. Hirschfeld, Phys. Today **68** 6, 46 (2015).
[16] R. M. Fernandes, A. V. Chubukov, and J. Schmalian, Nat. Phys. **10**, 97 (2014).
[17] J. Yang, R. Zhou, L. L. Wei, H. X. Yang, J. Q. Li, Z. X. Zhao, and G.-q. Zheng, Chin. Phys. Lett. **32**, 107401 (2015).
[18] S. Lederer, Y. Schattner, E. Berg, and S. A. Kivelson, Phys. Rev. Lett. **114**, 097001 (2015).
[19] Z.-X. Li, F. Wang, H. Yao, and D.-H. Lee, Science bulletin **61**, 925 (2016).
[20] S. Lederer, Y. Schattner, E. Berg, and S. A. Kivelson, Proc. Natl. Acad. Sci. U.S.A. **114**, 4905 (2017).
[21] C. M. Varma, K. Miyake, and S. Schmitt-Rink, Phys. Rev. Lett. **57**, 626 (1986).
[22] B. J. Ramshaw, S. E. Sebastian, R. D. McDonald, J. Day, B. S. Tan, Z. Zhu, J. B. Betts, R. X. Liang, D. A. Bonn, W. N. Hardy, and N. Harrison, Science **348**, 317 (2015).
[23] P. Walmsley, C. Putzke, L. Malone, I. Guillamon, D. Vignolles, C. Proust, S. Badoux, A. I. Coldea, M. D. Watson, S. Kasahara, Y. Mizukami, T. Shibauchi, Y. Matsuda, and A. Carrington, Phys. Rev. Lett. **110**, 257002 (2013).
[24] D. R. Parker, M. J. Pitcher, P. J. Baker, I. Franke, T. Lancaster, S. J. Blundell, and S. J. Clarke, Chem. Commun. **16**, 2189 (2009).
[25] See Supplemental Material at http://link.aps.org/supplemental/10.1103/PhysRevLett.121.167004 for additional data and analysis, that includes [26–35].

[26] Z. Li, D. L. Sun, C. T. Lin, Y. H. Su, J. P. Hu, and G.-q. Zheng, Phys. Rev. B **83,** 140506 (2011).

[27] F. L. Ning, K. Ahilan, T. Imai, A. S. Sefat, R. Y. Jin, M. A. McGuire, B. C. Sales, and D. Mandrus, J. Phys. Soc. Jpn. **78,** 013711 (2009).

[28] L. Luan, T. M. Lippman, C. W. Hicks, J. A. Bert, O. M. Auslaender, J. H. Chu, J. G. Analytis, I. R. Fisher, and K. A. Moler, Phys. Rev. Lett. **106,** 067001 (2011).

[29] B. S. Chandrasekhar and D. Einzel, Ann. Phys. (Berlin) **505,** 535 (1993).

[30] J. M. Luttinger, Phys. Rev. **119,** 1153 (1960).

[31] S. Ideta, T. Yoshida, I. Nishi, A. Fujimori, Y. Kotani, K. Ono, Y. Nakashima, S. Yamaichi, T. Sasagawa, M. Nakajima, K. Kihou, Y. Tomioka, C. H. Lee, A. Iyo, H. Eisaki, T. Ito, S. Uchida, and R. Arita, Phys. Rev. Lett. **110,** 107007 (2013).

[32] H. Shishido, A. F. Bangura, A. I. Coldea, S. Tonegawa, K. Hashimoto, S. Kasahara, P. M. C. Rourke, H. Ikeda, T. Terashima, R. Settai, Y. Onuki, D. Vignolles, C. Proust, B. Vignolle, A. McCollam, Y. Matsuda, T. Shibauchi, and A. Carrington, Phys. Rev. Lett. **104,** 057008 (2010).

[33] S. K. Yip and J. A. Sauls, Phys. Rev. Lett. **69,** 2264 (1992).

[34] S. Sridhar and J. E. Mercereau, Phys. Rev. B **34,** 203 (1986).

[35] A. F. Wang, J. J. Ying, X. G. Luo, Y. J. Yan, D. Y. Liu, Z. J. Xiang, P. Cheng, G. J. Ye, L. J. Zou, Z. Sun, and X. H. Chen, New J. Phys. **15,** 043048 (2013).

[36] E. H. Brandt, Phys. Rev. B **37,** 2349 (1988).

[37] S. Ghannadzadeh, J. D. Wright, F. R. Foronda, S. J. Blundell, S. J. Clarke, and P. A. Goddard, Phys. Rev. B **89,** 054502 (2014).

[38] S. Oh, A. M. Mounce, J. A. Lee, W. P. Halperin, C. L. Zhang, S. Carr, and P. Dai, Phys. Rev. B **87,** 174517 (2013).

[39] N. J. Curro, C. Milling, J. Haase, and C. P. Slichter, Phys. Rev. B **62,** 3473 (2000).

[40] V. F. Mitrović, E. E. Sigmund, M. Eschrig, H. N. Bachman, W. P. Halperin, A. P. Reyes, P. Kuhns, and W. G. Moulton, Nature (London) **413,** 501 (2001).

[41] G.-q. Zheng, H. Ozaki, Y. Kitaoka, P.Kuhns, A. P. Reyes, and W. G. Moulton, Phys. Rev. Lett. **88,** 077003 (2002).

[42] K. Kakuyanagi, K. Kumagai, Y. Matsuda, and M. Hasegawa, Phys. Rev. Lett. **90,** 197003 (2003).

[43] E. H. Brandt, Phys. Rev. Lett. **66,** 3213 (1991).

[44] D. R. Harshman, E. H. Brandt, A. T. Fiory, M. Inui, D. B. Mitzi, L. F. Schneemeyer, and J. V. Waszczak, Phys. Rev. B **47,** 2905 (1993).

[45] P. G. de Gennes, *Superconductivity of Metals and Alloys* (Westview Press, Oxford, 1999).

[46] E. Pardo, D.-X. Chen, and A. Sanchez, J. Appl. Phys. **96,** 5365 (2004).

[47] Z. H. Liu, P. Richard, K. Nakayama, G. F. Chen, S. Dong, J. B. He, D. M. Wang, T. L. Xia, K. Umezawa, T. Kawahara, S. Souma, T. Sato, T. Takahashi, T. Qian, Y. B. Huang, N. Xu, Y. B. Shi, H. Ding, and S. C. Wang, Phys. Rev. B **84,** 064519 (2011).

[48] Q. Q. Ge, Z. R. Ye, M. Xu, Y. Zhang, J. Jiang, B. P. Xie, Y. Song, C. L. Zhang, P. C. Dai, and D. L. Feng, Phys. Rev. X **3,** 011020 (2013).

[49] D. R. Parker, M. J. P. Smith, T. Lancaster, A. J. Steele, I. Franke, P. J. Baker, F. L. Pratt, M. J. Pitcher, S. J. Blundell, and S. J. Clarke, Phys. Rev. Lett. **104,** 057007 (2010).

[50] T. Okada, H. Takahashi, Y. Imai, K. Kitagawa, K. Matsubayashi, Y. Uwatoko, and A. Maeda, Physica (Amsterdam) **494C,** 109 (2013).

[51] D. Chowdhury, J. Orenstein, S. Sachdev, and T. Senthil, Phys. Rev. B **92,** 081113 (2015).

[52] T. Nomoto and H. Ikeda, Phys. Rev. Lett. **111,** 167001 (2013).

[53] A. Levchenko, M. G. Vavilov, M. Khodas, and A. V. Chubukov, Phys. Rev. Lett. **110,** 177003 (2013).

[54] D. Chowdhury, B. Swingle, E. Berg, and S. Sachdev, Phys. Rev. Lett. **111,** 157004 (2013).

[55] F. L. Ning, K. Ahilan, T. Imai, A. S. Sefat, M. A. McGuire, B. C. Sales, D. Mandrus, P. Cheng, B. Shen, and H. H. Wen, Phys. Rev. Lett. **104,** 037001 (2010).

[56] T. Moriya, J. Magn. Magn. Mater. **100,** 261 (1991).

[57] J. Korringa, Physica (Amsterdam) **16,** 601 (1950).

[58] H. Luetkens, H.-H. Klauss, M. Kraken, F. J. Litterst, T. Dellmann, R. Klingeler, C. Hess, R. Khasanov, A. Amato, C. Baines, M. Kosmala, O. J. Schumann, M. Braden, J. Hamann-Borrero, N. Leps, A. Kondrat, G. Behr, J. Werner, and B. Büchner, Nat. Mater. **8,** 305 (2009).

[59] G. Lang, L. Veyrat, U. Gräfe, F. Hammerath, D. Paar, G. Behr, S. Wurmehl, and H.-J. Grafe, Phys. Rev. B **94,** 014514 (2016).

[60] V. K. Thorsmølle, M. Khodas, Z. P. Yin, C. L. Zhang, S. V. Carr, P. C. Dai, and G. Blumberg, Phys. Rev. B **93,** 054515 (2016).

[61] Y. Schattner, S. Lederer, S. A. Kivelson, and E. Berg, Phys. Rev. X **6,** 031028 (2016).

[62] R. Daou, J. Chang, D. LeBoeuf, O. Cyr-Choiniere, F. Laliberte, N. Doiron-Leyraud, B. J. Ramshaw, R. X. Liang, D. A. Bonn, W. N. Hardy, and L. Taillefer, Nature (London) **463,** 519 (2010).

[63] Y. Sato, S. Kasahara, H. Murayama, Y. Kasahara, E. G. Moon, T. Nishizaki, T. Loew, J. Porras, B. Keimer, T. Shibauchi, and Y. Matsuda, Nat. Phys. **13,** 1074 (2017).

[64] L. Zhao, C. A. Belvin, R. Liang, D. A. Bonn, W. N. Hardy, N. P. Armitage, and D. Hsieh, Nat. Phys. **13,** 250 (2017).